



Regular article

Two-step flash sintering of ZnO: Fast densification with suppressed grain growth



Jiuyuan Nie, Yuanyao Zhang, Jonathan M. Chan, Sicong Jiang, Rongxia Huang, Jian Luo *

Department of NanoEngineering, University of California, San Diego, La Jolla, CA 92093, USA

ARTICLE INFO

Article history:

Received 19 June 2017

Received in revised form 14 July 2017

Accepted 14 July 2017

Available online xxxx

Keywords:

Sintering

Two-step sintering

Flash sintering

ZnO

Microstructure control

ABSTRACT

Two-step flash sintering (TSFS) was proposed as a new ceramic fabrication method to achieve fast densification with suppressed grain growth. Using ZnO as an exemplar, ~96.5% of theoretical density was achieved using TSFS with a grain size of ~370 nm, representing a >3 times reduction of the grain size in comparison with conventional (one-step) flash sintering. Moreover, TSFS achieved this result in a few minutes, >200 times faster than that needed for conventional two-step sintering to obtain comparable results, thereby representing an opportunity for significant energy and cost savings.

© 2017 Acta Materialia Inc. Published by Elsevier Ltd. All rights reserved.

In 2000, Chen and Wang developed an innovative two-step sintering method to inhibit the final-stage grain growth that would normally occur when the relative density is above ~90% [1]. In two-step sintering, a green specimen was first heated to a higher temperature, T_1 , to reach a critical relative density, followed by holding at a lower temperature, T_2 ($T_2 < T_1$), in the second step for a prolonged time to achieve a high relative density while suppressing the final-stage rapid grain growth. This method has been successfully applied to various ceramic materials, including undoped/doped Y_2O_3 [1,2], $BaTiO_3$ [3,4], ZnO [5], Al_2O_3 [6], and SiC [7]. Yet, there are several technical challenges for the application of two-step sintering. For example, a prolonged holding time in the second step, e.g., up to 20 h in the case of conventional two-step sintering of ZnO [5], is typically required. Moreover, the short holding duration in the first step and (sometimes) desired fast cooling from the first to second step [2,3,8] may lead to large relative deviations of the exact specimen temperatures from the targeted profiles. Inspired by a novel flash sintering method developed by Raj and co-workers in 2010 [9], here we proposed and subsequently demonstrated a new two-step flash sintering (TSFS) method to achieve comparable results as those demonstrated in conventional two-step sintering of ZnO [5] in as short as ~5 min; this represents a >200 times reduction in the sintering time [5], thereby implying not only convenient electronic controls (with ultrafast heating and cooling rates) but also a great potential for energy and cost savings with a drastically improved efficiency.

Flash sintering enabled fast densification at low furnace temperatures, which have been successfully applied to Y_2O_3 -stabilized ZrO_2 [9,

10], Y_2O_3 [11], ZnO [12–14], TiO_2 [15,16], $SrTiO_3$ [17,18], and other oxide [19–21] as well as non-oxide [22–25] ceramics. In most systems, the flash starts as a thermal runaway, where quantitative models [12, 13,15,26–28] have been developed and tested. At least for ZnO, fast densification is related to ultrahigh heating rates (~200 °C/s) since a recent study demonstrated that rapid thermal annealing with comparable heating profiles can achieve similar densification and grain growth rates [13]. However, rapid final-stage grain growth also occurred in flash sintering in a similar fashion as those observed in conventional sintering, albeit a much shorter time scale [13]. In this study, we further proposed a new TSFS method to substantially reduce the final-stage grain growth as compared with the conventional (one-step) flash sintering and subsequently demonstrated its feasibility using a model system (ZnO).

A ZnO powder (99.95% purity, purchased from US Research Nanomaterials, Inc.) was mixed with 0.5 wt% binder (PVA in DI water). The mixtures were uniaxially pressed at ~300 MPa to form green pellets of the dimension: D (diameter) = 6.4 mm and H (height) = 2.8 mm. Green pellets were baked at 500 °C for 1 h to burn out the binder. After burning the binder, the average grain size in the green pellets was measured to be 36 ± 2 nm and the bulk densities were measured to be $57.3 \pm 0.8\%$. The specimen surfaces were sputtered with platinum as electrodes using a Denton Discovery 18 Sputtering System. The sides of the sputtered specimens were ground using SiC papers. For flash sintering experiments, specimens were loaded into a modified dilatometer (DIL 402 PC, Netzsch, Boston, MA, USA) equipped with Pt electrodes and circuit (for applying electric fields/currents) and flowed with argon at a constant rate of 33 mL/min. The system was purged with argon for 1 h before heating up to 500 °C at a

* Corresponding author.

E-mail address: jluo@alum.mit.edu (J. Luo).

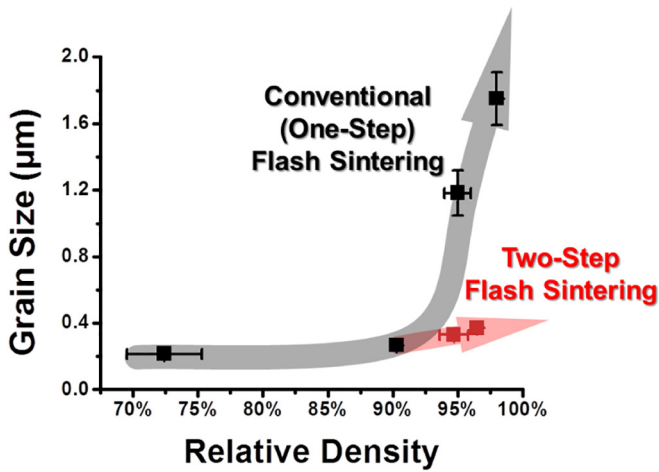


Fig. 1. Grain size vs. relative density of ZnO specimens fabricated by one-step and two-step flash sintering.

constant rate of 5 °C/min. Subsequently, the flash sintering experiments were conducted isothermally at 500 °C, where a programmable DC power supply (DLM300–10, Ametek Inc., San Diego, CA, USA) was used to apply electric fields/currents.

All flash sintering experiments were conducted at an isothermal furnace temperature of $T_F = 500$ °C in this study (instead of a constant ramping rate as in most other flash sintering experiments, so that it can be better compared with TSFS experiments), where a flash typically started ~20–30 s after applying the constant (initial) electric field of $E_{\text{initial}} = 150$ V/cm. The electric field was kept a constant (150 V/cm in this case), until the specimen current reached a preset limit and the power supply was switched from a voltage-control to a current-control mode. For conventional (one-step) flash sintering, the current limit (I_{max}) was kept at 3 A (corresponding to a nominal current density of $J_{\text{max}} \approx 95$ mA/mm², calculated from the initial specimen dimension; noting that the actual J_{max} increased with time due the densification of specimen) for a duration of 2 s, 6 s, 15 s, and 30 s, respectively, after the onset of flash. For TSFS, the current limit was set to $I_1 = 3$ A

(nominal $J_1 \approx 95$ mA/mm²) for a fixed duration of 6 s (3 A × 6 s) in the first step and subsequently reduced to $I_2 = 2$ A (nominal $J_2 \approx 63$ mA/mm²) and kept for a duration of 150 s or 300 s. After flash sintering, both the electric power and the furnace were shut down and the specimens were cooled down in the furnace; the flowing argon was shut off after the specimen cooled to room temperature.

After the completion of flash sintering experiments, the specimen densities were calculated *via* measuring dimensions and weights; the Archimedes method was also used if the relative densities were >90%. Microstructures of flash sintered specimens were characterized using a field-emission ultra-high resolution environmental scanning electron microscope (UHR-SEM, FEI XL30) operating at 10 kV. Grain sizes were measured from SEM micrographs of fractured surfaces using a standard intercept method.

The grain size vs. relative density curves for both conventional (one-step) flash sintering and TSFS are shown in Fig. 1. Representative microstructures of the fractured surfaces of six sintered specimens are shown in Fig. 2. Here, the grain sizes and densities were measured from specimens that were cooled down to room temperature, where the effects of the densification and grain growth during the cooling were also included.

In conventional (one-step) flash sintering experiments, the relative density increased from ~57% in the green specimen to ~72% in the 3 A × 2 s sintered specimen, while the grain size increased from 36 ± 2 nm in the green specimen to 214 ± 18 nm in the sintered specimen. Increasing the flash sintering duration from 2 s to 6 s, the relative density increased substantially to ~90%, while the grain size increased only moderately to 267 ± 30 nm, in the 3 A × 6 s sintered specimen. Further increasing the flash sintering duration, the relative density increased to ~95% with a substantial grain growth to 1.18 ± 0.14 μm in the 3 A × 15 s sintered specimen; the relative density and grain size, respectively, reached ~97.6% and 1.75 ± 0.16 μm, respectively, in the 3 A × 30 s sintered specimen. Here, the observed rapid final-stage grain growth (when the relative density was above ~90%) is consistent with results measured from conventional flash sintering, as well as rapid thermal annealing, of ZnO conducted in air [13] and it agrees with what is expected from the classical sintering theory.

The linear shrinkage was also measured *in situ* by dilatometry for flash sintering of ZnO at 500 °C in argon ($E_{\text{initial}} = 150$ V/cm and

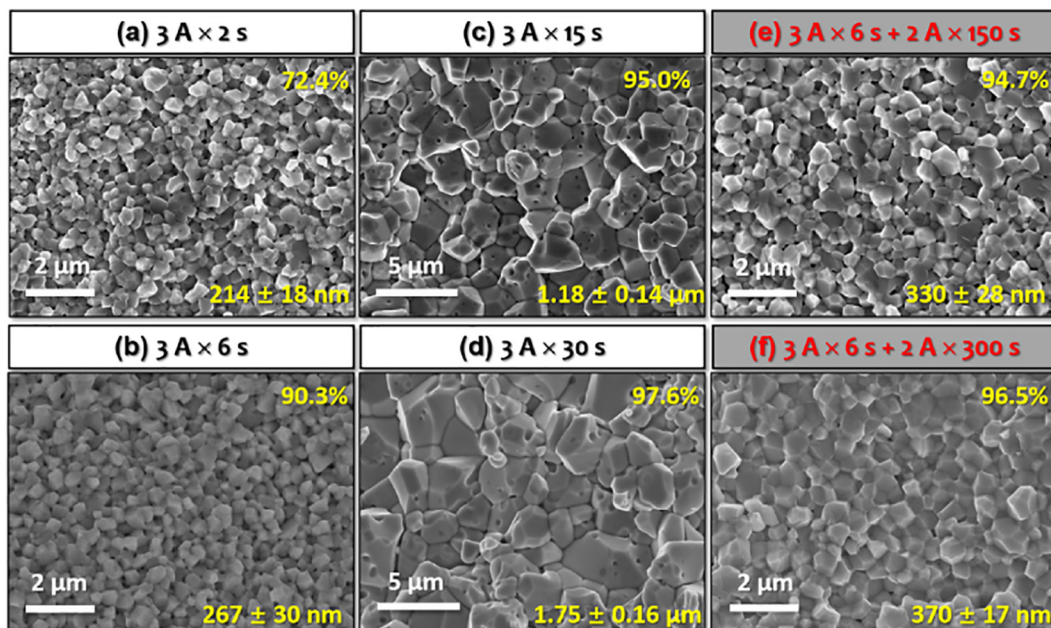


Fig. 2. SEM micrographs of the fractured surfaces of the conventional (one-step) flash sintered ZnO specimens quenched (a) 2 s, (b) 6 s, (c) 15 s, and (d) 30 s, respectively, after the onset of flash, where the current limits were 3 A, as well as the two-step flash sintered ZnO specimens quenched after (e) 3 A × 6 s + 2 A × 150 s and (f) 3 A × 6 s + 2 A × 300 s.

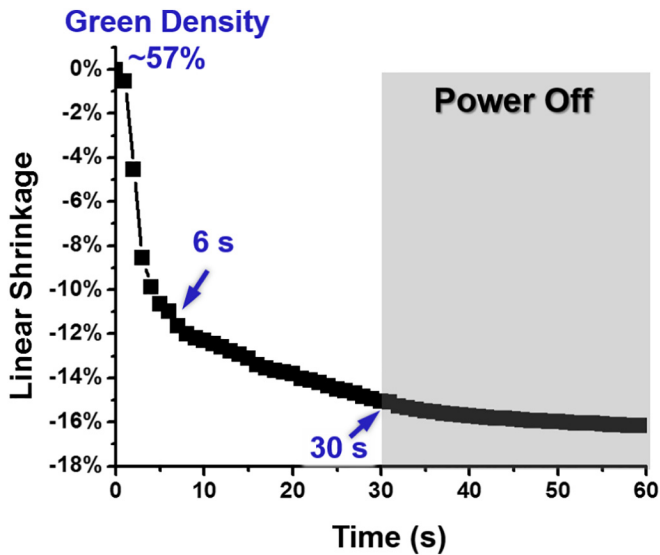


Fig. 3. Measured linear shrinkage vs. time curve for (one-step) flash sintering of ZnO conducted in argon with a constant furnace temperature of $T_F = 500^\circ\text{C}$, where the applied electric field was set to 150 V/cm initially and the maximum current limit was set to 3 A. Electric power was shut off 30 s after the onset of flash (while the densification continues for ~30 s during the cooling of the specimen).

$I_{\text{max}} = 3\text{ A}$), where electric power was shut off at 30 s after the onset of flash (Fig. 3). The specimen densified to ~93% in 30 s after the onset of flash as measured by *in-situ* dilatometry. The final density was measured using the Archimedes method to be 97.6% (close to that calculated from the measured linear shrinkage at 60 s). This measured linear shrinkage vs. time curve was used as a guide to select the duration for the first step of the TSFS experiments to be 6 s, at which time the specimen reached ~81% of the theoretical density, since a prior study of conventional two-step sintering of ZnO suggested that the first step should reach to >78% of theoretical density [5]. Noting the measured relative density of the $3\text{ A} \times 6\text{ s}$ sintered specimen was ~90%, which included the contribution of densification during the cooling.

In the TSFS (i.e., two-step flash sintering) experiments conducted with $E_{\text{initial}} = 150\text{ V/cm}$, a fixed first step of $3\text{ A} \times 6\text{ s}$ (i.e., $I_1 = 3\text{ A}$ for a fixed duration of 6 s), and a second step at a reduced current of $I_2 = 2\text{ A}$ for a longer duration of 150 s, the grain size only increased to $330 \pm 28\text{ nm}$ with a further increase in the relative density to 94.7% (in comparison with the ~267 nm grain size and ~90% density of the $3\text{ A} \times 6\text{ s}$ sintered specimen; see Fig. 1 and Fig. 2). A longer second step of 300 s resulted in a grain size of $370 \pm 17\text{ nm}$ and a relative density of 96.5% in the $3\text{ A} \times 6\text{ s} + 2\text{ A} \times 300\text{ s}$ sintered specimen. As shown in Fig. 1, the grain growth was suppressed in the TSFS experiments, where the grain sizes were <1/3 of those expected in the conventional (one-step) flash sintering with identical densities from interpolation. The grain size vs. density curve obtained from the TSFS was similar to that of the optimal case of conventional two-step sintering of ZnO reported in a prior study [5]; yet TSFS achieved this result (~370 nm grain size at ~96.5% relative density) in ~5 min, whereas it took ~15–20 h in conventional two-step sintering to achieve comparable results of densification and grain growth (i.e., ~500 nm at ~95% or ~650 nm at ~98% relative density, with a smaller starting particle/grain size of ~11 nm) [5]. In other words, the new TSFS method is >200 times faster in obtaining comparable (or slightly better) results than the conventional two-step sintering [5], representing a substantial opportunity for energy and cost savings *via* drastically improving the efficiency.

We also conducted a $2\text{ A} \times 600\text{ s}$ one-step flash sintering experiment for an additional comparison, which produced a 95.6% dense specimen with the measured average grain size of $2.01 \pm 0.18\ \mu\text{m}$ (Supplementary Fig. S1). This result suggested that longer holding at 2 A could not achieve the simultaneous small grain size and high density obtained by the TSFS.

The measured time-dependent current, current density, electric field, and linear shrinkage of a representative specimen undergoing TSFS (in the first ~35 s after the flash) are shown in Fig. 4(a)–(d). The calculated power density and estimated specimen temperature (T_s) from the blackbody radiation model [12] are shown in Fig. 4(e) and (f). The actual current followed the controlled profile ($3\text{ A} \times 6\text{ s} + 2\text{ A} \times 300\text{ s}$) well with only minor fluctuations, while the relatively large fluctuations in the voltage (electric field) vs. time curve reflected the specimen response under the current-control mode. While the current

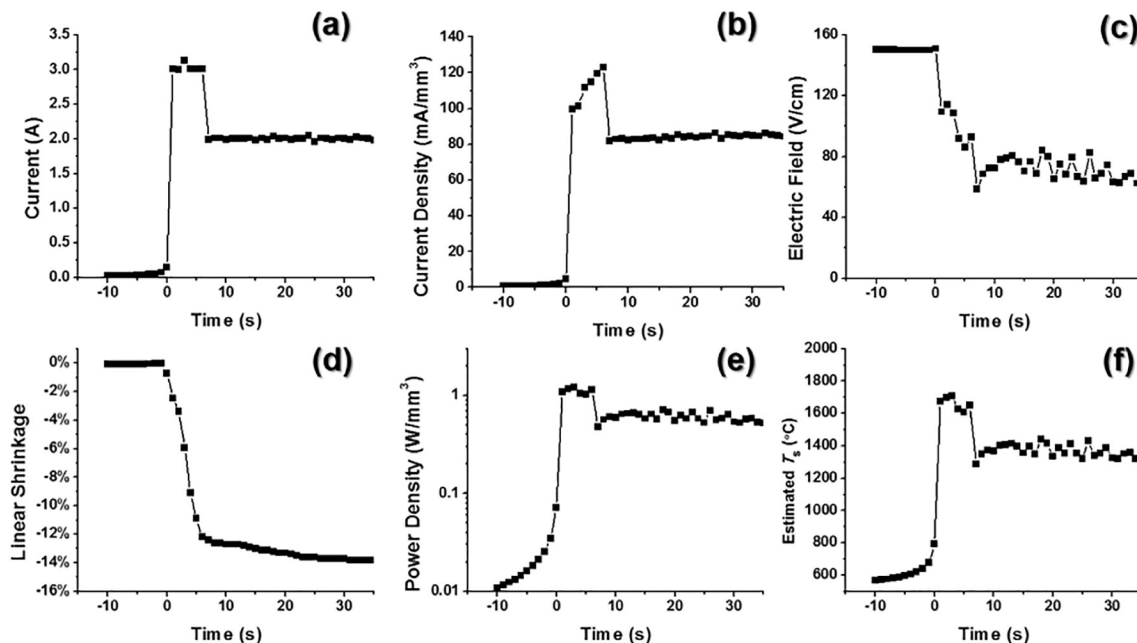


Fig. 4. *In-situ* measurements of the first ~35 s in TSFS, including time-dependent (a) current, (b) current density, (c) electric field, and (d) linear shrinkage, as well as the (e) computed power density and (f) estimated specimen temperature (T_s).

was controlled to be a constant in each step (Fig. 4(a)), the current density increased continuously (more noticeably in the first step) due to the specimen shrinkage during densification (Fig. 4(b)). It was evident from the measured linear shrinkage vs. time curve (Fig. 4(d)) that densification was fast in the first step (0 to 6 s) and slowed down in the second step. The power density increased gradually in the incubation period under the voltage-control mode prior to the onset of the flash, but it largely followed a two-step function in the TSFS under the current-control mode (Fig. 4(e)). The estimated specimen temperature (T_s) was between 1600 and 1700 °C in the first step and between 1300 and 1450 °C in the second step; thus, the temperature difference (ΔT_s) between the two steps was estimated to be ~200–300 °C (Fig. 4(f)). The final relative density of the $3 \text{ A} \times 6 \text{ s} + 2 \text{ A} \times 300 \text{ s}$ sintered specimen (after cooling to room temperature) was measured to be $96.5 \pm 0.3\%$ using the Archimedes method and the grain size was measured to be $370 \pm 17 \text{ nm}$.

In summary, a new TSFS method has been proposed to achieve fast densification (in comparison with the conventional two-step sintering) with suppressed grain growth (in comparison with the conventional flash sintering), where a specimen was kept at a higher current of I_1 for a short duration t_1 after the onset of flash, and electronically switched to a lower current of $I_2 (< I_1)$ for a longer duration $t_2 (> t_1)$. Using ZnO as a model system, this study successfully achieved ~96.5% of the theoretical density with a grain size of ~370 nm (representing a >3 times reduction in final-stage grain growth in comparison with the conventional one-step flash sintering) in ~5 min using this new TSFS method, which is >200 times faster than that can be obtained in the conventional two-step sintering. This cost-effective and energy-saving TSFS method can potentially be applied on other materials to achieve fast densification with suppressed grain growth. This study further suggests a new direction to control the densification and microstructural evolution *via* controlling and manipulating the $I(t)$ profile in flash sintering to any preset profile to achieve better or more customized results.

This work is supported by the Aerospace Materials for Extreme Environments program of the U.S. Air Force Office of Scientific Research (AFOSR) under the grant no. FA9550-14-1-0174. We gratefully thank our AFOSR program manager, Dr. Ali Sayir, for his support and guidance.

Supplementary data to this article can be found online at <http://dx.doi.org/10.1016/j.scriptamat.2017.07.015>.

References

- [1] I.W. Chen, X.H. Wang, Nature 404 (6774) (2000) 168–171.
- [2] X.H. Wang, P.L. Chen, I.W. Chen, Journal of the American Ceramic Society 89 (2) (2006) 431–437.
- [3] X.H. Wang, X.Y. Deng, H.L. Bai, H. Zhou, W.G. Qu, L.T. Li, I.W. Chen, J. Am. Ceram. Soc. 89 (2) (2006) 438–443.
- [4] T. Karaki, K. Yan, T. Miyamoto, M. Adachi, Japanese Journal of Applied Physics Part 2-Letters & Express Letters 46 (4–7) (2007) L97–L98.
- [5] M. Mazaheri, A.M. Zahedi, S.K. Sadmezhaad, J. Am. Ceram. Soc. 91 (1) (2008) 56–63.
- [6] J.G. Li, Y.P. Ye, J. Am. Ceram. Soc. 89 (1) (2006) 139–143.
- [7] Y.I. Lee, Y.W. Kim, M. Mitomo, D.Y. Kim, J. Am. Ceram. Soc. 86 (10) (2003) 1803–1805.
- [8] M. Mazaheri, A. Simchi, F. Golestani-Fard, J. Eur. Ceram. Soc. 28 (15) (2008) 2933–2939.
- [9] M. Cologna, B. Rashkova, R. Raj, J. Am. Ceram. Soc. 93 (11) (2010) 3556–3559.
- [10] M. Cologna, A.L. Prette, R. Raj, J. Am. Ceram. Soc. 94 (2) (2011) 316–319.
- [11] H. Yoshida, Y. Sakka, T. Yamamoto, J.-M. Lebrun, R. Raj, J. Eur. Ceram. Soc. 34 (4) (2014) 991–1000.
- [12] Y.Y. Zhang, J.I. Jung, J. Luo, Acta Mater. 94 (2015) 87–100.
- [13] Y.Y. Zhang, J.Y. Nie, J.M. Chan, J. Luo, Acta Mater. 125 (2017) 465–475.
- [14] C. Schmerbauch, J. Gonzalez-Julian, R. Röder, C. Ronning, O. Guillon, J. Am. Ceram. Soc. 97 (6) (2014) 1728–1735.
- [15] Y.Y. Zhang, J.Y. Nie, J. Luo, J. Ceram. Soc. Jpn. 124 (4) (2016) 296–300.
- [16] S.K. Jha, R. Raj, J. Am. Ceram. Soc. 97 (2) (2014) 527–534.
- [17] F. Lemke, W. Rheinheimer, M.J. Hoffmann, Scr. Mater. 130 (2017) 187–190.
- [18] A. Karakuscu, M. Cologna, D. Yarotski, J. Won, J.S. Francis, R. Raj, B.P. Uberuaga, J. Am. Ceram. Soc. 95 (8) (2012) 2531–2536.
- [19] X. Hao, Y. Liu, Z. Wang, J. Qiao, K. Sun, J. Power Sources 210 (2012) 86–91.
- [20] A. Gaur, V.M. Sglavo, Journal of Materials Science 49 (18) (2014) 6321–6332.
- [21] A.L. Prette, M. Cologna, V. Sglavo, R. Raj, J. Power Sources 196 (4) (2011) 2061–2065.
- [22] E. Zapata-Solvas, S. Bonilla, P. Wilshaw, R. Todd, J. Eur. Ceram. Soc. 33 (13) (2013) 2811–2816.
- [23] S. Grasso, T. Saunders, H. Porwal, B. Milsom, A. Tudball, M. Reece, J. Am. Ceram. Soc. (2016).
- [24] Y.H. Dong, I.W. Chen, J. Am. Ceram. Soc. 99 (9) (2016) 2889–2894.
- [25] S. Grasso, T. Saunders, H. Porwal, O. Cedillos-Barraza, D.D. Jayaseelan, W.E. Lee, M.J. Reece, J. Am. Ceram. Soc. 97 (8) (2014) 2405–2408.
- [26] R.I. Todd, E. Zapata-Solvas, R.S. Bonilla, T. Sneddon, P.R. Wilshaw, J. Eur. Ceram. Soc. 35 (6) (2015) 1865–1877.
- [27] Y. Dong, I.W. Chen, J. Am. Ceram. Soc. 98 (8) (2015) 2333–2335.
- [28] Y. Dong, I.W. Chen, J. Am. Ceram. Soc. 98 (12) (2015) 3624–3627.